IEEE Access
Multidisciplinary ⋮ Rapid Review ⋮ Open Access Journal

Received May 27, 2021, accepted June 6, 2021, date of publication June 9, 2021, date of current version June 18, 2021.

Digital Object Identifier 10.1109/ACCESS.2021.3087782

Early Detection of Pediatric Seizures in the High Gamma Band

MICHELLE DEDEO[1,2], (Member, IEEE), AND MAANASI GARG[3]
[1]Department of Mathematics and Statistics, Jacksonville, FL 32224, USA
[2]Mayo Clinic, Jacksonville, FL 32224, USA
[3]Management and Technology, University of Pennsylvania, Philadelphia, PA 19104, USA

Corresponding author: Michelle DeDeo (mdedeo@unf.edu)

ABSTRACT Using data from the MIT Physionet EEG database collected at the Children's Hospital Boston, we identify a method of detecting seizures in ten pediatric patients at least thirty seconds before seizure onset by identifying significant preictal locations and their respective frequencies within the high gamma band of 30 through 100 Hz. We analyze the potential predictive performance of event-related potential analysis in this high gamma band, provide evidence that detection algorithms should take into account the varying strength of a patient's common frequency extremes, and provide evidence that patient-specific approaches to machine learning algorithms may be more successful in the detection of pediatric seizures as they are more difficult to detect than adult seizures. Using these results, machine learning detection algorithm performance on pediatric patient data, which is prone to issues from limitations within the algorithms, may be significantly improved by incorporating high gamma band signal processing at the locations identified by this process.

INDEX TERMS Biomedical engineering, biomedical signal processing, computational systems biology, encephalography.

I. INTRODUCTION

A. BACKGROUND

Epileptic seizures, caused by excessive synchronization of large neural groups, affect 1% of the population [1]. Of these patients, 30% have seizures that are resistant to anti-epileptic drugs [1], also known as intractable seizures. Current treatment options available for intractable epilepsy include surgical resection and neuromodulation techniques. However, not all patients are appropriate candidates for surgical procedures, and neuromodulation has been observed to give few patients freedom from seizures [1], [2]. Most studies attempt to address the need for more specific detection methods and little success has been made with pediatric seizures [3]. In addition, most studies are limited to between 4 and 21 patients due to the difficulty of obtaining reliable data sets for multiple patients [4], [5].

Analysis types used to evaluate EEG data can be either statistical or algorithmic. For a better understanding of the practical problems in this field, early studies were categorized [4], [5] on seizure prediction and detection according to methodological standards along with relevant characteristics (type of epilepsy and EEG, type of EEG analysis, number of patients and seizures, amount of data analyzed, etc.). Significant electrical changes can be subtle and difficult to identify through observation of an electroencephalogram (EEG) recording. To overcome these obstacles, various univariate and multivariate statistical measures have been used for EEG analysis including wavelet transforms, entropy measures, phase correlation, and synchronization measures [2].

Despite the importance of information visualization in modern data analysis, few papers exploring preictal analysis extend their data analysis to include visualizations. By combining power frequency analysis of preictal epochs with visual analysis of preictal patterns to explore possibilities of seizure detection, we are able to observe patterns in the data without compromising data integrity [6].

Here we analyze the potential predictive performance of event-related potential (ERP) analysis in the high gamma band, provide evidence that detection algorithms should take into account the varying strength of a patient's common frequency extremes (CFEs), as defined below, and provide evidence that patient-specific approaches to machine learning algorithms may be more successful in seizure prediction than patient-specific approaches [3]. We note that some researchers contest the validity of gamma wave activity

The associate editor coordinating the review of this manuscript and approving it for publication was Yizhang Jiang.

detected by scalp EEG due to the fact that the frequency band of gamma waves overlaps the electromyographic frequency band. As this study shows, the high gamma band is relevant in pediatric seizure detection.

B. PRIOR STUDIES

Prior to 2002, studies commonly focused entirely on preictal periods and did not include an evaluation of interictal control recordings. In the early 2000's, another group of studies tackled the issue of specificity by comparing preictal changes in dynamics to interictal control recordings. Initial controlled studies defined groups of patients with preictal and interictal control recordings and evaluated measures such as correlation dimension, dynamical entrainment, accumulated signal energy, simulated neuronal cell models and phase synchronization were shown to be suitable for distinguishing interictal from preictal data. Around 2003, a number of studies were published that challenged the reliability of correlation dimension, dynamical entrainment, and accumulated signal energy [7].

Seizure detection algorithms are prone to issues that arise from limitations within the algorithms. For example, in 2012 Dalton *et al.* [5] developed and studied a body sensor network that monitors and detects epileptic seizures based on statistics extracted from time-domain signals. These statistics include the mean, variance, zero-crossing rate, entropy, and auto-correlation with template signals. The sensitivity of the proposed algorithm for a data set of 21 seizures with five patients is found to be 91% with a specificity of 84% but yielded a fairly high rate of 50 false positives.

In 2018, Zhou *et al.* [3] compared the performances of time and frequency domain signals in the detection of epileptic signals based on the intracranial Freiburg and the pediatric MIT Physionet EEG database (CHB-MIT) [8] collected at the Children's Hospital Boston (CHB) used in this study. Using time domain signals in the Freiburg database, the average accuracies were 91.1, 83.8, and 85.1% in their experiments, while the signal detection accuracies in the pediatric CHB-MIT database were only 59.5, 62.3, and 47.9%, respectively. This underscores similar results that effective identification using time domain signals as input samples is achieved for only some pediatric patients.

In 2019, Zhang *et al.* [9] used convolutional neural networks (CNN) to distinguish between the preictal state and the interictal state in the frequency range of 5 to 50 Hz. Their model showed performance with a sensitivity of 92.2% and false prediction rate of 0.12/h, however they augment the preictal trials by splitting each training EEG trial into three segments, and then generate new artificial trials as a concatenation of segments coming from diverse and randomly selected training trials of the preictal state.

Machine learning methods such as CNN and support vector machine (SVM) cannot achieve high sensitivity and low false prediction rate (FPR) simultaneously. The additional signal identifiers found in this paper may not only be useful in helping machine learning algorithms improving detection accuracy while alleviating the use of artificial trials.

II. METHODS

A. STUDY-SPECIFIC FREQUENCY ANALYSIS

Frequency analysis of ictal and preictal EEG recordings have been used and proven as an effective technique to analyze preictal epochs [2]. Frequency analysis consists of breaking down a time signal into its composing sinusoidal waves and which allows for analysis of the main frequencies which constitute the time signal. Event-related potential analysis can be used to analyze time-locked electric potential patterns immediately following a stimulus [10]. In this study, ERP imaging is used to explore electric potential patterns preceding the stimulus of seizure onset.

Previous frequency analysis studies have proposed a correlation between high frequency spectral activity and seizure onset. However, there is no agreement across various studies for the definition of ''high frequency'' [11]–[16]. Papers that do identify high frequency oscillations (HFOs) as a feature of preictal periods identify activity in broad frequency ranges that vary from 40 to 140 Hz and 100 to 500 Hz [12], [14]. HFOs ranging between 80 and 500 Hz have been recorded during interictal [17], [18], preictal [19] and ictal [20] periods. These disparate ranges hinder comparison of studies as they do not provide a concrete frequency range correlating with seizure onset.

Here we focus on EEG frequency analysis in the band commonly defined in the high gamma range between 30 and 100 Hz. This range covers the most common upper gamma band interval used in EEG analysis and may help solidify a concrete relationship between high frequencies and preictal activity. We note there is a debate on whether scalp EEG information is appropriate as these recordings often reveal spontaneous high frequency EEG components such as sustained gamma and induced gamma, which increase with visual, memory or sensorimotor tasks [21], [22]. It has long been assumed that scalp EEG is heavily influenced by electromyogram activity and various methods attempt to remove its influence have been devised as in the evoked response methodology [23].

B. DATA AND PATIENT INFORMATION

The MIT Physionet EEG database [24], collected at the Children's Hospital Boston, published continuous scalp EEG recordings for 23 pediatric intractable seizure patients using the International 10–20 montage system [8] using longitudinal bipolar montages, i.e. every channel displays the voltage measured at one electrode in reference to the voltage measured at another position [25]. The implications of analyzing bipolar channels rather than unipolar channels are discussed below. The Physionet database is a part of PhysioBank, a large and growing archive of well-characterized digital recordings of physiological signals and related data for use by the biomedical research community.

Each individual patient data set contains between 9 and 42 hours continuous recording. In order to protect the privacy

of the subjects, all protected health information in the original files have been replaced with bipolar signals. For the purposes of this study, the 23 patients in the database were narrowed down to a group of 10 patients which meet the following selection criteria: 1) the patient had at least 5 ictal and 5 interictal EEGs recorded; 2) the patient recordings included all recorded channel and bipolar montage locations; and 3) the patient had relatively artifact-free EEG recordings [26]. The 10 selected patients (Patients 3, 5, 8, 10, 14, 16, 18, 20 and 23, respectfully) included 8 females and 2 males ranging from the ages of 3 to 18. All EEG recordings were sampled at a frequency of 256 Hz with 16-bit resolution. Anti-seizure medications had been withdrawn from the patients prior to beginning of the EEG recordings.

For a given patient, the spectral character of seizures within the EEG is similar from one seizure to the next provided that the seizures originate from the same cerebral site(s). It is important to distinguish this work from investigations using intracranial EEGs or machine-learning to detect seizures. Methods that process intracranial EEG rely on features that cannot be observed within the scalp EEG because of the spatial averaging effect of the dura and skull. Intracranial EEG is immune to corruption by artifacts (e.g. scalp muscle contractions) that can mask the onset of seizure activity within the scalp EEG. Although this is the ideal method for studying seizures, intracranial EEGs require invasive surgery.

For each patient, five ictal epochs, five 30-second preictal epochs, and five random interictal epochs were extracted from the patient's EEG recordings for a total of 150 epochs (15 per patient). Increasing epoch duration increases spectral resolution. As in other studies, we define an ictal epoch as a recording encompassing a full seizure with at least 6 to 10 seconds of length. Data from the ictal epoch were only used to time-stamp the intervals and are not otherwise used in the study. For this study, an interictal epoch is defined as a randomly chosen, artifact-free 90-second period.

We note that epochs with significant artifacts were excluded from the study and that any remaining artifacts such as eye movement, speech, chewing or tongue movement, pulse, moving, electrode ''pop'', etc. do not affect the results of the study due to the statistical impossibility ($< .01\%$) of the same artefact occurring at the same time for each patient over multiple EEGs as well as the consistency of the preictal and ictal activity at each individual frequency over multiple EEGs for each patient.

C. FEATURE EXTRACTION

The method for feature extraction, feature selection and post-processing included spectral power computation and spectral power ratio computation using EEGLAB [27] toolbox for Matlab 9.7. The time-frequency analysis options of EEGLAB allow calculation of event-related spectral perturbation which reflects the extent to which the power at different frequencies in a signal is altered in relation to a specific time point such as signal onset. Power spectral analysis, the foundation of frequency analysis [28], is used to determine which gamma band frequencies contributed the most power during patient seizure ''electrical surges'' relative to their non-seizure periods. Power spectral density (PSD) graphs the density of the power of a signal as a function of frequency [26], [29]. Using PSD, estimates of each patient's ictal and interictal epochs were compared to assess which gamma band frequencies contributed the most power during the ictal periods.

Power spectral density calculations rely on the Fourier transform since any function can be represented as a combination of sinusoidal waves with various frequencies and amplitudes. The Fourier transform of a time-domain function creates a frequency domain representation of the same function. The frequency domain representation represents the amplitudes of each frequency in the frequency spectrum that must be added to obtain the original function. The discrete Fourier transform is defined as the following:

$$\hat{x}(t) = \int_{-\infty}^{\infty} x(t) e^{-2\pi i t f}\, dt$$

where $\hat{x}(t)$ is the Fourier transform of $x(t)$. Given that t is a function of microvolts over time, $|x(t)|^2$ is a function of the instantaneous power of the signal over time with unit resistance. The following represents the average power of the signal:

$$AvePower = \lim_{T\to\infty} \frac{1}{T} \int_0^T |x(t)|^2\, dt$$

where $x(t)$ is the time length of the signal. According to Parseval's theorem, the integral of the square of a function is equal to the integral of its Fourier transform:

$$AvePower = \lim_{T\to\infty} \int_0^T \frac{\left|\hat{x}(f)\right|^2}{T} df$$

where $\frac{|\hat{x}(f)|^2}{T}$ is the spectral density of $x(t)$. PSD calculations for each epoch were then computed using Welch's method of power spectral density estimation as Welch's method usually involves less computation than other PSD methods. Welch's method divides the time signal into successive blocks, forming the periodogram for each block, and then averaging [30]. In window-based signal processing, the input signal, $s(t)$ is divided into input segments and the signal is processed segment by segment. Let M denote the lengths of each segment and L denote the total number of segments. Let $s_l = s(n + (l-1)M/2)$ for $n = 0, \ldots, M-1$ and $l = 1, \ldots, L$ denote the windowed signal in the l^{th} segment. The main advantage of the window-based signal processing is that the number of observation points computed is reduced by a factor of $M/2$ as compared to sample-by-sample processing.

Each epoch is divided into 10 segments of the same size with 50% overlap for each epoch. Each segment is then windowed with a Hamming window. We use the discrete Fast Fourier Transform (FFT) to create a modified periodogram for each segment. The FFT requires a dataset that is 2^N elements long, i.e. 2, 4, 8, 16, 32, etc., so the transform uses

the value of N that is closest to the signal length (nFFT). The modified periodograms were averaged to obtain the power spectral density estimate of the epoch [19, 22]. It should be noted that if the input signal cannot be divided into an integer number of components, the signal is truncated accordingly.

To compute the (absolute) spectral power in the frequency bands, the PSD of the input signal is estimated. The PSD of a signal, $s(n)$ describes the distribution of the signal's total average power over frequency. For this paper, the spectral power P_i of a signal in a frequency band is computed as the logarithm of the sum of the PSD coefficients within each frequency band. The spectral power for window-based processing in the i^{th} frequency band is computed as

$$P_i = log \sum_{w \in Band(i)} PSD_i(w)$$

for $i = 1, \ldots, 10$ where $P(l)$ is a time series whose l^{th} element represents the spectral power of the l^{th} input signal in the segment in Band i. This procedure is used to estimate the PSD at each of the 18 EEG recording channels for each patient during their ictal and interictal epochs. During the ictal events, EEG activities are largely obscured by muscle and movement artifacts which can make it difficult to differentiate a genuine seizure from a pseudo-seizure. Thus we use the fact that presence of post-ictal flattening or slowing provides evidence of a genuine seizure [31].

Preictal and interictal EEG patterns across patients vary substantially. The preictal data segment preceding the seizure onset can range from a few seconds to several hours long [32]. To determine the start of the ictal event, the rhythmic activity associated with the onset of a seizure is often composed of multiple frequency components. Thus to determine the onset of a seizure, multiple spectral components were considered. The spectral content of a seizure epoch may overlap the dominant frequency of an epoch of non-seizure activity. As the presence or absence of other spectral components distinguishes them, expert visual marking combined with EEGLAB's event detector denoted the start of each ictal event. Although the current the gold standard for seizure onset is expert visual marking, the LOO (Leave-One-Patient-Out) or First Seizures models of Gomez et al [33] may supersede this standard.

Since an EEG cannot be segmented into short physiologically relevant units, two second long epochs are commonly used. We extract the spectral structure of a sliding window of length $L = 2$ seconds by passing it through a filter bank composed of $M = 8$ filters, and then measuring the energy falling within the passband of each filter. Although increasing the number of filters does not greatly impact how quickly a detector recognizes the onset of a seizure, the increase helps better discriminate between seizure and non-seizure states.

To automatically capture the spectral and spatial information contained within each two second EEG epoch at time $T = t$, we concatenate the $M = 8$ spectral energy extracted from each of $N = 18$ EEG channels. This process forms a feature vector X_t with $M \times N = 144$ elements.

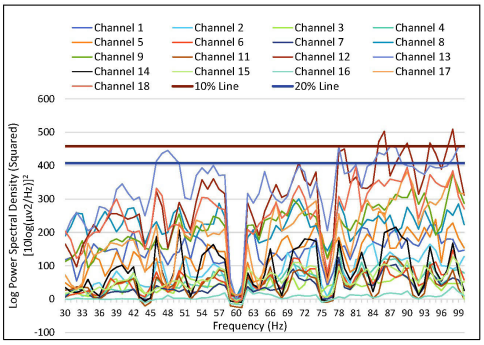

FIGURE 1. Patient 1 (11-year old female). One of five 30-second preictal epoch of the average-squared power spectral densities (PSDs). Eighteen channel frequencies measured before a seizure with upper 10% and upper 20% log-power spectral densities by channel and frequency denoted. Excluded values are represented by sharp valleys at 60 and 76 Hz.

Electroencephalographers require an EEG abnormality to persist and evolve for a minimum of 6 to 10 seconds before considering the abnormality a seizure or a component of a seizure. Taking this into account, we form a stacked feature vector from X_T that results from concatenating the feature vectors from 3 contiguous, but non-overlapping, 2 second epochs so that the classifier considers the evolution of feature vectors over a period of 6 seconds.

For each patient, the average difference between the PSD of each ictal epoch and the PSDs of the five interictal epochs is calculated separately for each of the 18 EEG recording channels. Five graphs were created for each patient depicting the squared magnitudes of their average log-power differences. For each of the five graphs, the top 20% common frequency extremes of their average log-power squared values over all frequencies and bipolar locations of each patient's individual preictal episode over the respective preictal event were recorded (Figures 1 and 2).

The resulting common extreme frequency values and their respective ratio in the upper 20% threshold were recorded for each patient (Figure 3). The resultant extrema signified gamma band frequencies that contributed to abnormally high power during most of a patient's ictal epochs is recorded. These common extreme frequency values for each patient are referred to as CFEs and the bipolar channel location number of the common extremes are referred to as BCNs. We note that main drawback of using spectral powers is the high false positive ratio (FPR) as the PSD increases often in the interictal periods as well. False positives were not observed in the data in this study as the probability of a false positive over five separate epochs at the same frequency is statistically improbable ($<.01\%$).

We note that a band-pass filter is used to eliminate 60 Hz and 76 Hz activity as power line noise occurs at 60 Hz and since the third harmonic of 60 Hz which is 180Hz can be aliased to 76 Hz when a sampling rate of 256Hz is used. Thus data between the frequencies of 59 to 61 Hz and 75 to 77 Hz are, as such, dismissed. We also note that Figures 1 and 2 show a small dip at 44 Hz which is most likely the fifth harmonic of 300 Hz which is aliased to 44 Hz. Also, the third

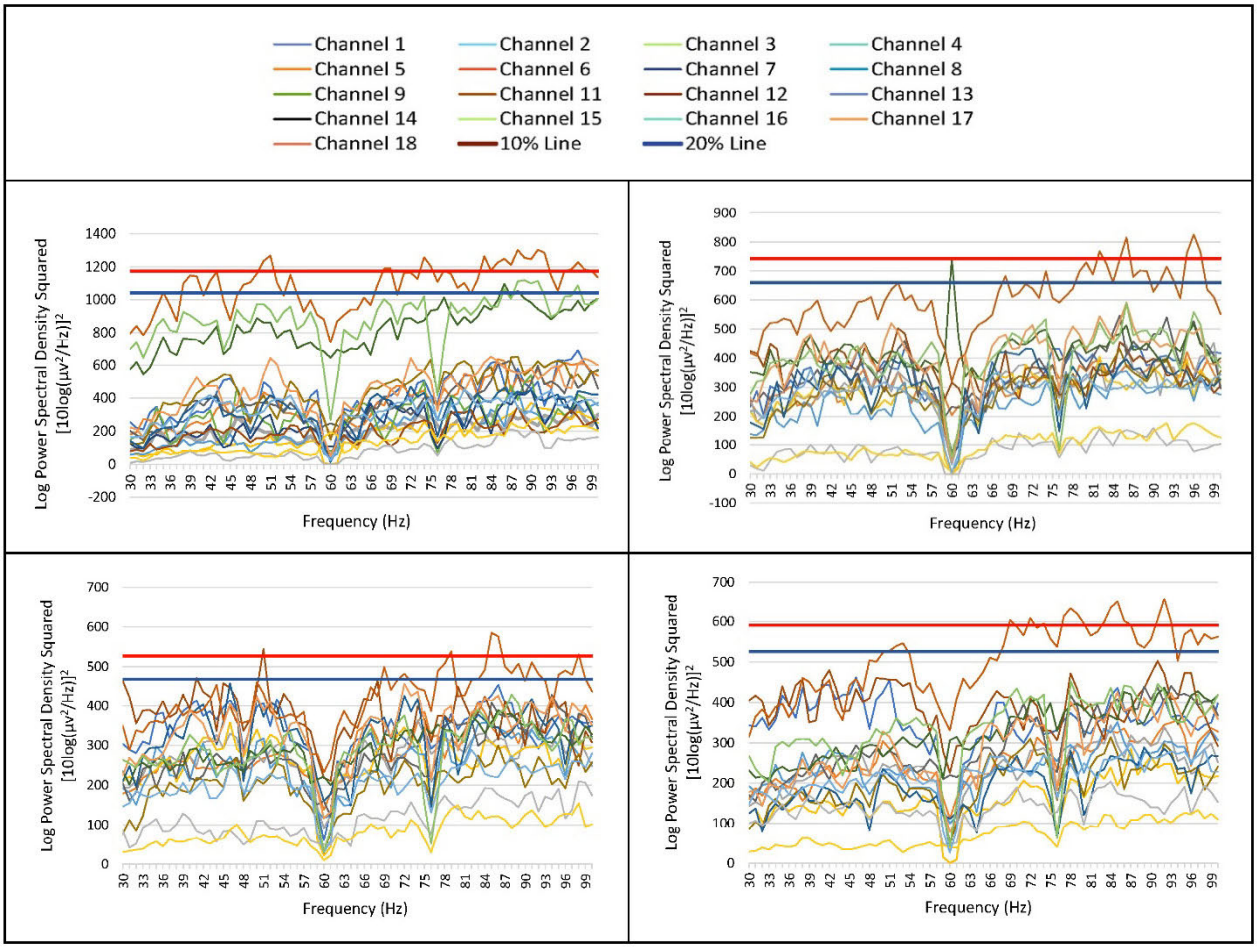

FIGURE 2. Patient 8 (18-year old female). Four of five thirty-second preictal epochs of average-squared power spectral densities. Eighteen channels measured 30 seconds before a seizure with upper 10% and upper 20% log-power spectral densities by channel and frequency denoted. Note that the preictal Log Power scale shifts for each epoch. Excluded values are represented by sharp valleys at 60 and 76 Hz.

harmonic of 20 Hz can also be seen when sampling at 200 Hz aliasing 180 Hz to 20 Hz. We note that odd harmonics are more often seen than even harmonics in EEG studies.

III. RESULTS

Nine of the 10 patients were found to have CFEs in the high gamma band range between 70 Hz and 100 Hz (Table 1, Figure 3). The only frequency outlier is Patient 3 who had CFEs of 39 Hz and 54 Hz. Since each patient had focal seizures in different brain areas, there is no significant overlap with the BCNs (bipolar channel number) for each patient as expected [7]. Eight of the nine relevant patients were found to have significantly denser activity between $\pm$[5,10] μV at the 70 Hz to 100 Hz CFEs in preictal epochs in comparison to their interictal epochs (Figures 4, 5, and 6). This indicates that the buildup of 70 to 100 Hz activity is a distinguishing feature of preictal epochs. Patient 4 is the only patient of the nine patients to have no significant difference between preictal and interictal epoch activity at its high gamma CFEs.

The data frequency outlier, Patient 3, did not show the same pattern differences as other patients between preictal and interictal epochs at 39 Hz and 54 Hz CFEs (Figure 6).

TABLE 1. Patient common frequency extremes (CFEs) with their respective channel and bipolar channel location number (BCN).

Patient No.	Channel	BCN	CFE(s)
1	12	P4-O2	90, 97, 98 Hz
	13	FP2-F8	78, 87 Hz
2	13	FP2-F8	72 Hz
	14	F8-T8	72 Hz
3	14	F8-T8	39, 54 Hz
4	18	CZ-PZ	83, 86, 90 Hz
5	18	CZ-PZ	85, 90, 98 Hz
	13	FP2-F8	93 Hz
6	13	FP2-F8	93 Hz
	18	CZ-PZ	99 Hz
7	15	T8-P8	87, 90 Hz
8	13	FP2-F8	85, 86 Hz
9	2	F7-T7	95 Hz
	12	P4-O2	93, 94, 98, 99 Hz
10	1	FP1-F7	89, 93, 94 Hz

However, when ERP images were created of Patient 3's preictal and interictal epochs at random frequencies between 70 Hz and 100 Hz, the patient's data followed the pattern as the other patients. In other words, all of the patient's preictal epochs at frequencies between 70 and 100 Hz and at the respective BCNs corresponding with the patient's actual CFEs had

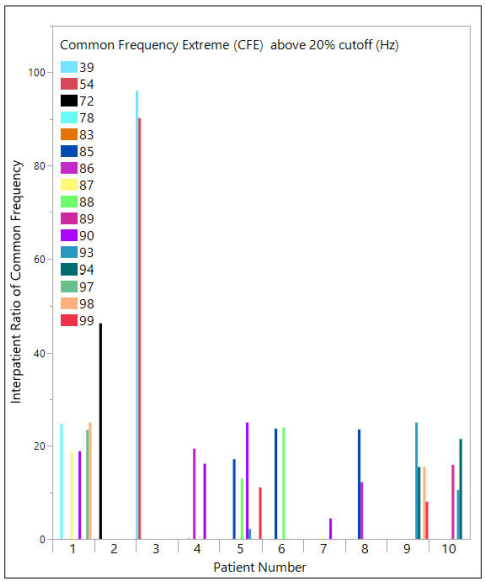

FIGURE 3. Ratio (%) of common frequency extremes (CFEs) of all 10 patients above 20% cutoff. Note: Twenty-eight of the 30 CFEs (93%) lie in the high gamma band between 70 and 100Hz.

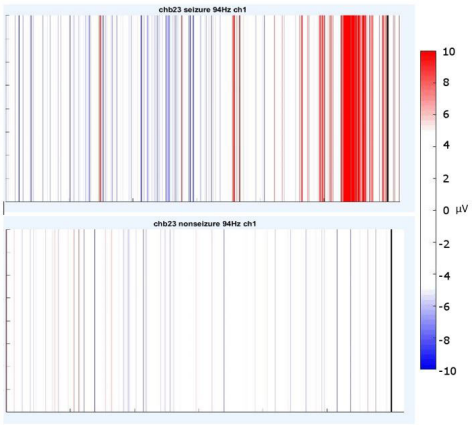

FIGURE 4. Patient 10 (6-year old female). One of five preictal (top) and interictal (bottom) ERP images at bipolar montage channel 1 (FP1-F7) at 94Hz over 30-second intervals.

significantly denser activity between ±[5,10] μV in comparison to the interictal epochs. Thus despite Patient 3's low CFEs values (39 and 54Hz), their activity within 70 and 100 Hz frequencies still served as the distinguishing feature of their preictal epochs.

A. TECHNICAL VALIDATION

For each of a patient's five preictal epochs, voltage at the first CFE and its corresponding BCN is represented by a color-coded rectangle. The five resulting colored rectangles were vertically stacked upon each other. A Gaussian vertically moving average is then used to smooth the stacked rectangle colors into single vertical lines.

Finally, the color map is changed to a two-color red and blue scale with the top quartile of the voltage scale represented in red and the bottom quartile in blue. The middle quartiles were considered insignificant as they reflect normal

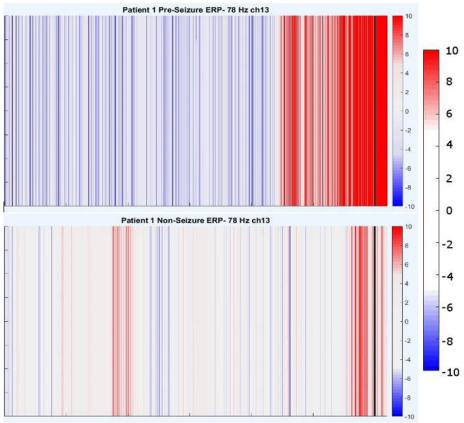

FIGURE 5. Patient 1 (11-year old female). One of five preictal (top) and interictal (bottom) ERP images at bipolar montage channel 13 (FP2-F8) at 78Hz over 30-second intervals.

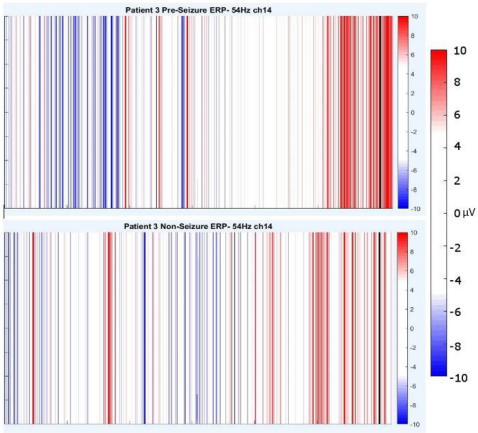

FIGURE 6. Patient 3 (7-year old female) - Outlier. One of five preictal ERP (top) and interictal (bottom) ERP images at bipolar montage channel 14 at 54Hz over 30-second intervals. Although no visual differences are detected between preictal and ictal ERP images at 54Hz, the activity ratio at channel 14 was 90.2% higher than the value at the 20% cutoff line (see Figure 3).

brain activity and were set to white. This process is used to create an ERP Image of each patient's thirty-second preictal epochs at each of the patient's CFEs and corresponding BCNs. These images were then compared to ERP images of the individual patient's interictal epochs at the same CFEs and corresponding BCNs (Figures 4, 5, 6). We note that the ERP images of the interictal epochs were also thirty seconds in length, so the original 90-second interictal epochs were shortened to their middle 30 seconds for direct comparison. The preictal ERP images and interictal ERP images are then compared using data visualization at each scale to explore possible preictal patterns using color coding a scale of [-10,10] μV with ±10 μV representing the extremes in brain activity at a given bipolar scalp location.

B. DATA AVAILABILITY

A team of investigators from Children's Hospital Boston and the Massachusetts Institute of Technology created and contributed the database to PhysioNet [24]. All raw data is available online [8] and all datasets and analyses used in this paper are available on figshare [34]. The EEG recordings of

TABLE 2. Script to estimate the mean power for a specific lead which uses the entire available time window, compute log spectrum for different frequencies and find the average power within the predefined frequency. EEGLAB's spectopo function uses Matlab's pwelch function whose values can be adjusted to suit further studies.

```
sampRate = xxx; % sampling rate of the data
lowerFreq = 30; % lower bound of the frequency band of interest
higherFreq = 100;  % upper bound of the frequency band
chanNr = xx;  % channel number of the lead
sampWin = 101:500;  % indices of sample points used in analysis
(if empty, whole segment is used)
% computing log spectrum for different frequencies
if isempty(sampWin)
[power, freq] = spectopo(EEG.data(chanNr, :), 0, sampRate);
else
[power, freq] = spectopo(EEG.data(chanNr, sampWin), 0, sampRate);
end
% average power within the predefined frequency range
meanPower = mean(power(freq ≥ lowerFreq & freq ≤ higherFreq));
```

the Children's Hospital Boston recordings used a longitudinal bipolar montage to insure patient confidentiality. We note that the use of bipolar channels does not invalidate the power spectral density analysis or ERP analysis performed on the channel data [7], [29].

C. CODE AVAILABILITY

Initial analysis, computations and ERP images (Figures 4, 5 and 6) were completed with the University of California – San Diego. All relevant documentation are available online [27]. The script in Table 2 estimates the mean power for a specific lead which uses the entire available time window. We note that EEGLAB's spectopo function uses Matlab's pwelch function and that the values below are arbitrary numbers which can be adjusted to suit further studies. Figures 1, 2, and 3 were created using EEGLAB lab data exported into Excel.

IV. DISCUSSION

We note that the 70 to 100 Hz range is usually ignored in scalp EEG as recorders often have filters that start attenuating the signal at 70 Hz to reduce aliasing when the signal is digitized so that signals above 70 Hz have lower voltage. It has been suggested that only subdural recordings that are sampled at 1000 samples per second or higher give reliable data at these higher frequencies, but the data in this study suggest that this may not be the case. Distinct ictal activity is found in the frequency range between 70 and 100 Hz. This prompts exploration of whether this activity is a result of, or a cause of, the ictal epochs. If preictal activity is found to be a cause of the ictal epochs, medical reduction of 70 to 100 Hz brain activity before the onset of a seizure may help prevent the seizure or, at the minimum, reduce its severity.

Considerations include the fact that that preictal and interictal patterns vary substantially between patients and that preictal and interictal patterns may vary substantially from seizure to seizure, and from hour to hour, within a single patient. Thus patient-specific approaches yield better seizure detection performance. The results of this study also show that the issues listed above are not a concern as the patients' EEGs in this study were analyzed using extensive signal processing techniques and, of the 50 preictal epochs analyzed (five pre-seizure episodes per patient), 50 interictal epochs (5 non-seizure episodes per patient) and 50 ictal epochs (5 seizure episodes per patient), evidence of preictal seizure activity occurred in every preictal epoch in 9 of 10 patients. This degree of accuracy would not occur if spontaneous high frequency EEG components were involved. Limitations include the use of pediatric EEG data and the number of patients in the study as the choice of patients evaluated is designed to avoid the use of patient data with excessive artifacts.

A. FURTHER RESEARCH

In addition to utilizing these results to supplement machine learning algorithms such as CNN, SVM, dynamical similarity index, mean phase coherence, phase-locking value, zero-crossings, Gaussian mixture and other models, we suggest that a direct extension of this study would be to apply the same type of PSD analysis and visualization techniques to non-pediatric seizure patients as well as determine a consensus in the literature on a frequency ranges for seizure detection. This could establish whether the patterns found in this study applies only to all intractable seizure patients. We also recommend that these techniques be applied to preictal periods longer than thirty seconds to determine the beginning of the increased preictal activity in the patients. In addition, further study could be done to identify the possible contribution of EMG to scalp EEG rhythms at rest and induced or evoked by cognitive tasks as well as the undertaking of more studies of this type in the gamma band.

ACKNOWLEDGMENT

With thanks to the team of investigators from Children's Hospital Boston and the Massachusetts Institute of Technology that contributed the database to PhysioNet [24]. The clinical investigators from CHB include Jack Connolly, REEGT; Herman Edwards, REEGT; Blaise Bourgeois, MD; and S. Ted Treves, MD. The authors also acknowledge the reviewers' feedback and recommendations.

REFERENCES

[1] D. J. Englot, J. D. Rolston, C. W. Wright, K. H. Hassnain, and E. F. Chang, "Rates and predictors of seizure freedom with vagus nerve stimulation for intractable epilepsy," *Neurosurgery*, vol. 79, no. 3, pp. 345–353, 2016, doi: 10.3171/2011.7.JNS11977.

[2] P. R. Carney, S. Myers, and J. D. Geyer, "Seizure prediction: Methods," *Epilepsy Behav.*, vol. 22, pp. S94–S101, Dec. 2011, doi: 10.1016/j.yebeh.2011.09.001.

[3] M. Zhou, C. Tian, R. Cao, B. Wang, Y. Niu, T. Hu, H. Guo, and J. Xiang, "Epileptic seizure detection based on EEG signals and CNN," *Frontiers Neuroinform.*, vol. 12, p. 95, Dec. 2018, doi: 10.3389/fninf.2018.00095.

[4] T. N. Alotaiby, S. A. Alshebeili, T. Alshawi, I. Ahmad, and F. E. A. El-Samie, "EEG seizure detection and prediction algorithms: A survey," *EURASIP J. Adv. Signal Process.*, vol. 2014, no. 1, pp. 1–21, Dec. 2014, doi: 10.1186/1687-6180-2014-183.

[5] A. Dalton, S. Patel, A. R. Chowdhury, M. Welsh, T. Pang, S. Schachter, G. Olaighin, and P. Bonato, "Development of a body sensor network to detect motor patterns of epileptic seizures," *IEEE Trans. Biomed. Eng.*, vol. 59, no. 11, pp. 3204–3211, Nov. 2012, doi: 10.1109/TBME.2012.2204990.

[6] C. Friedman, Y. Liu, Y. Lussier, and Y. Tao, "Information visualization techniques in bioinformatics during the postgenomic era," *Drug Discovery Today, BIOSILICO*, vol. 2, no. 6, pp. 237–245, 2004, doi: 10.1016/s1741-8364(04)02423-0.
[7] F. Mormann, R. G. Andrzejak, C. E. Elger, and K. Lehnertz, "Seizure prediction: The long and winding road," *Brain*, vol. 130, no. 2, pp. 314–333, Feb. 2007, doi: 10.1093/brain/awl241.
[8] A. L. Goldberger, L. A. N. Amaral, L. Glass, J. M. Hausdorff, P. C. Ivanov, R. G. Mark, J. E. Mietus, G. B. Moody, C.-K. Peng, and H. E. Stanley, "PhysioBank, PhysioToolkit, and PhysioNet: Components of a new research resource for complex physiologic signals," *Circulation*, vol. 101, no. 23, pp. e215–e220, 2000, doi: 10.1161/01.CIR.101.23.e215.
[9] Y. Zhang, Y. Guo, P. Yang, W. Chen, and B. Lo, "Epilepsy seizure prediction on EEG using common spatial pattern and convolutional neural network," *IEEE J. Biomed. Health Informat.*, vol. 24, no. 2, pp. 465–474, Feb. 2020, doi: 10.1109/JBHI.2019.2933046.
[10] A. H. Shoeb and J. V. Guttag, "Application of machine learning to epileptic seizure detection," in *Proc. ICML*, 2010, pp. 975–982. [Online]. Available: https://icml.cc/Conferences/2010/papers/493.pdf
[11] G. Alarcon, C. D. Binnie, R. D. Elwes, and C. E. Polkey, "Power spectrum and intracranial EEG patterns at seizure onset in partial epilepsy," *Electroencephalogr. Clin. Neurophysiol.*, vol. 94, no. 5, pp. 326–337, 1995, doi: 10.1016/0013-4694(94)00286-T.
[12] C. Alvarado-Rojas, M. Valderrama, A. Fouad-Ahmed, H. Feldwisch-Drentrup, M. Ihle, C. A. Teixeira, F. Sales, A. Schulze-Bonhage, C. Adam, A. Dourado, S. Charpier, V. Navarro, and M. Le Van Quyen, "Slow modulations of high-frequency activity (40–140 Hz) discriminate preictal changes in human focal epilepsy," *Sci. Rep.*, vol. 4, no. 1, pp. 1–9, May 2015, doi: 10.1038/srep04545.
[13] S. Arroyo and S. Uematsu, "High-frequency EEG activity at the start of seizures," *J. Clin. Neurophysiol.*, vol. 9, no. 3, pp. 441–448, Jul. 1992, doi: 10.1097/00004691-199207010-00012.
[14] A. Pearce, D. Wulsin, J. A. Blanco, A. Krieger, B. Litt, and W. C. Stacey, "Temporal changes of neocortical high-frequency oscillations in epilepsy," *J. Neurophysiol.*, vol. 110, no. 5, pp. 1167–1179, Sep. 2013, doi: 10.1152/jn.01009.2012.
[15] M. P. Richardson and J. G. R. Jefferys, "Introduction—Epilepsy research U.K. Workshop 2010 on 'preictal phenomena,"' *Epilepsy Res.*, vol. 97, no. 3, pp. 229–230, Dec. 2011, doi: 10.1016/j.eplepsyres.2011.10.027.
[16] G. A. Worrell, L. Parish, S. D. Cranstoun, R. Jonas, G. Baltuch, and B. Litt, "High-frequency oscillations and seizure generation in neocortical epilepsy," *Brain*, vol. 127, no. 7, pp. 1496–1506, Jul. 2004, doi: 10.1093/brain/awh149.
[17] A. Bragin, J. R. Engel, I. Fried, J. Staba, and C. L. Wilson, "Quantitative analysis of high frequency oscillations (80–500 Hz) recorded in human epileptic hippocampus and entorhinal cortex," *J. Neurophysiol.*, vol. 88, no. 4, pp. 1743–1752, 2002, doi: 10.1152/jn.2002.88.4.1743.
[18] E. Urrestarazu, R. Chander, F. Dubeau, and J. Gotman, "Interictal high-frequency oscillations (100–500 Hz) in the intracerebral EEG of epileptic patients," *Brain*, vol. 130, no. 9, pp. 2354–2366, Sep. 2007, doi: 10.1093/brain/awm149.
[19] J. Jacobs, R. Zelmann, J. Jirsch, R. Chander, C. E. Dubeau, and J. Gotman, "High frequency oscillations (80–500 Hz) in the preictal period in patients with focal seizures," *Epilepsia*, vol. 50, no. 7, pp. 92–1780, 2009, doi: 10.1111/j.1528-1167.2009.02067.x.
[20] J. D. Jirsch, "High-frequency oscillations during human focal seizures," *Brain*, vol. 129, no. 6, pp. 1593–1608, Apr. 2006, doi: 10.1093/brain/awl085.
[21] J.-P. Lachaux, E. Rodriguez, J. Martinerie, C. Adam, D. Hasboun, and F. J. Varela, "A quantitative study of gamma-band activity in human intracranial recordings triggered by visual stimuli," *Eur. J. Neurosci.*, vol. 12, no. 7, pp. 2608–2622, Jul. 2000, doi: 10.1046/j.1460-9568.2000.00163.x.
[22] C. Tallon-Baudry, "Oscillatory synchrony and human visual cognition," *J. Physiol. Paris*, vol. 97, nos. 2–3, pp. 355–363, Mar. 2003, doi: 10.1016/j.jphysparis.2003.09.009.
[23] E. M. Whitham, K. J. Pope, S. P. Fitzgibbon, T. Lewis, C. R. Clark, S. Loveless, M. Broberg, A. Wallace, D. DeLosAngeles, P. Lillie, A. Hardy, R. Fronsko, A. Pulbrook, and J. O. Willoughby, "Scalp electrical recording during paralysis: Quantitative evidence that EEG frequencies above 20 Hz are contaminated by EMG," *Clin. Neurophysiol.*, vol. 118, no. 8, pp. 1877–1888, Aug. 2007, doi: 10.1016/j.clinph.2007.04.027.
[24] *Physionet: The Research Resource for Complex Physiologic Signals*. MIT Laboratory for Computational Physiology. Accessed: Aug. 29, 2019. [Online]. Available: https://physionet.org/
[25] T. D. Lagerlund, "Manipulating the magic of digital EEG: Montage reformatting and filtering," *Amer. J. Electroneurodiagnostic Technol.*, vol. 40, no. 2, pp. 121–136, Jun. 2000, doi: 10.1080/1086508x.2000.11079295.
[26] T. Inouye, K. Shinosaki, H. Sakamoto, S. Toi, S. Ukai, A. Iyama, Y. Katsuda, and M. Hirano, "Quantification of EEG irregularity by use of the entropy of the power spectrum," *Electroencephalogr. Clin. Neurophysiol.*, vol. 79, no. 3, pp. 204–210, 1991, doi: 10.1016/0013-4694(91)90138-T.
[27] *EEGLAB: An Interactive MATLAB Toolbox*. UCSD Swartz Center for Computational Neuroscience. Accessed: Jul. 4, 2019. [Online]. Available: https://sccn.ucsd.edu/eeglab/
[28] K. K. Jerger, T. I. Netoff, J. T. Francis, T. Sauer, L. Pecora, S. L. Weinstein, and S. J. Schiff, "Early seizure detection," *J. Clin. Neurophysiol.*, vol. 18, no. 3, pp. 259–268, May 2001, doi: 10.1097/00004691-200105000-00005.
[29] C. E. Tenke, "Statistical characterization of the EEG: The use of the power spectrum as a measure of ergodicity," *Electroencephalogr. Clin. Neurophysiol.*, vol. 63, no. 5, pp. 488–493, 1986, doi: 10.1016/0013-4694(86)90131-8.
[30] P. Welch, "The use of fast Fourier transform for the estimation of power spectra: A method based on time averaging over short, modified periodograms," *IEEE Trans. Audio Electroacoust.*, vol. AU-15, no. 2, pp. 70–73, Jun. 1967, doi: 10.1109/TAU.1967.1161901.
[31] G. M. Galloway, *Clinical Neurophysiology in Pediatrics: A Practical Approach to Neurodiagnostic Testing and Management*. New York, NY, USA: Demos Medical, 2015.
[32] M. D. Haan and K. M. Thomas, "Applications of ERP and fMRI techniques to developmental science," *Develop. Sci.*, vol. 5, no. 3, pp. 335–343, Aug. 2002, doi: 10.1111/1467-7687.00373.
[33] C. Gómez, P. Arbeláez, M. Navarrete, C. Alvarado-Rojas, M. Le Van Quyen, and M. Valderrama, "Automatic seizure detection based on imaged-EEG signals through fully convolutional networks," *Sci. Rep.*, vol. 10, no. 1, pp. 1–13, Dec. 2020, doi: 10.1038/s41598-020-78784-3.
[34] M. DeDeo and M. Garg. (2021). Pediatric EEG data & analyses in high gamma band from boston children's hospital. Figshare. Dataset. [Online]. Available: https://doi.org/10.6084/m9.figshare.14044220.v3

MICHELLE DEDEO (Member, IEEE) received the M.S. degree in mathematics from California State University, Los Angeles, in 1991, and the M.A. and Ph.D. degrees in applied mathematics from the University of California at San Diego, in 1998. From 1998 to 2004, she was an Assistant Professor with the University of North Florida, Jacksonville. Since 2005, she has been an Associate Professor with the Department of Mathematics and Statistics. In 2017, she took on an additional role as a Research Collaborator with Mayo Clinic, Jacksonville. Her research interests include theoretical models of optimal computer networks, large data in the biomedical sciences, and applied data science. She has received numerous awards, including a Dean's Fellowship to analyze the socioeconomic effects of the opioid crisis in northeast Florida using the DEA's ARCOS database and grants, including a U.S. $1.6 million DOE grant, as a Co-PI. In 2020, she was a Keynote Speaker at the Third Annual Data Science, Analytics and Artifical Intelligence Conference, Boca Raton, FL, USA. Past projects include survival analysis on patients with glioblastoma, predicting seizures of pediatric patients from bipolar EEG data and serving as a Lead Advisor for the Florida Data Science for Social Good Program.

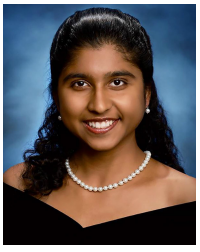

MAANASI GARG is currently pursuing the dual M&T degree with the School of Engineering and Applied Sciences and the Wharton School, University of Pennsylvania. In 2019, she was a Product Engineering Intern with Fairbanc, where she researched and developed POC for five class and hybrid computer vision AI models. She was a Regeneron International Science and Engineering Fair (ISEF) State Finalist and presented at the international competition for her work on seizure prediction in 2017. Her research interests include the integration of business and engineering by simultaneously considering of goals defined by management and engineering goals defined by the chief technical officers.